Journal of Applied Polymer Science

Rheology and Morphology of Nanosilica-Containing Polypropylene and Polypropylene/Liquid Crystalline Polymer Blend

Reza Foudazi, Hossein Nazockdast
Department of Polymer Engineering, Amirkabir University of Technology, Tehran, Iran
Correspondence to: R. Foudazi (E-mail: reza.foudazi@case.edu.)

ABSTRACT: We studied the rheology and morphology of hydrophilic and hydrophobic silica containing polypropylene (PP) and PP/liquid crystalline polymer (LCP) blend. It was found that hydrophilic silica has higher tendency for aggregation and forms bigger aggregate size. The lower percolation threshold and the higher fractal dimension for hydrophilic silica are due to its stronger particle–particle interaction compared with the hydrophobic one. Although the hydrophobic silica has lower thickening capability and lower coalescence hindrance by aggregates, its presence at the interface of PP/LCP blend results in smaller droplet size and higher elasticity of hybrid samples in comparison to hydrophilic silica. These results confirm that the hydrophobic silica has a compatibilization capability for PP/LCP blend, whereas the hydrophilic silica mostly works as a thickening agent and suppresses the coalescence. We suggested that for comparison of different particulate compatibilizers, the elasticity of filled blend sample against filled matrix phase can be used in high and low frequency ranges. © 2012 Wiley Periodicals, Inc. J. Appl. Polym. Sci. 000: 000–000, 2012

Received 6 January 2012; accepted 21 June 2012; published online
DOI: 10.1002/app.38269

INTRODUCTION

The presence of nanofillers in molten polymers results in significant change of viscoelastic properties. Consequently, melt linear viscoelastic behavior is a way generally used to assess the state of dispersion of nanocomposites directly in the melt state. During the past few years, intensive discussions have been hold on the rheology of polymer layered silicate nanocomposites, whereas the rheology of nanocomposites filled with spherical particles, and more particularly fumed silica, seems to have been received less attention. The particle–particle and particle–polymer interactions have a major impact on the rheological and reinforcement properties of fumed silica nanocomposites due to the large surface area of particles.[1–3] Fumed silica fillers have the potential for self-aggregation due to their fractal structure and high specific area, and hence they can form a network of connected or interacting particles in the molten polymer.[1–4]

The nanocomposites containing fumed silica show a solid-like behavior response at low deformation rates with following characteristics: a nonterminal zone of relaxation, apparent yield stress, and a shear-thinning dependence on viscosity at high deformation rates.[1] This particular rheological behavior arises from the presence of a network structure. This network structure can be formed by partly adsorption of polymer chains on the filler surface and partly entanglement with neighboring ones,[2] which give rise to a subset of stiffer chains extending from the interface, resulting in a dynamically stiffer matrix as well as a higher loss modulus due to an increase in hydrodynamic friction.[5] This finding was evidenced by viscoelastic experiments showing that the low frequency modulus of the composites decreases considerably when the particles are chemically treated with organosilane. However, the density of adsorbed chain (bound chain) and their conformation at the filler surface are generally quite difficult to access.[2,6]

Two mechanisms are presented in the literature to depict the solid-like behavior qualitatively: the particle–particle interaction is the dominant mechanism in fumed silica nanocomposites, whereas the particle–polymer interaction is the dominant one in colloidal silica nanocomposites at identical filler concentration. Obviously, these interactions are balanced in each nanocomposite systems by the silica surface treatment (chain grafting, silane modification) and the matrix characteristics.[1]

Polymer blends comprising of a flexible matrix and small amount of liquid crystalline polymers (LCP) are of industrial and academic interests because the dispersed LCP phase can lead to easier processing and enhanced mechanical properties (e.g. Refs. 7–9). Addition of compatibilizer has been found to improve the dispersion of the LCP phase and in some cases

enhance the final mechanical properties of the blend systems. Using a compatibilizer—which is compatible or miscible with both phases—is the classical route to ensure adhesion between two phases. For example the addition of maleic anhydride-grafted polypropylene (PP) as a compatibilizer to PP/LCP blends was studied by Datta and Baird[10] and O'Donnel and Baird.[11] The enhanced dispersion in compatibilized polymer blends is due to the reduction of interfacial tension and suppression of coalescence.[12]

Another less explored compatibilization method is that by use of inorganic solid particles.[13–15] Cassagnau and coworkers[16] studied the effect of both hydrophilic and hydrophobic nanosilica on PP/Polystyrene (PS) and PP/Ethylene vinyl acetate (EVA) blends[17] They showed that while the hydrophilic silica tends to locate inside PS phase in PP/PS blend, the hydrophobic silica preferentially concentrates at the interface and PP phase.[16] For PP/EVA blend samples, it was found that the hydrophilic silica tends to confine in the EVA phase, whereas hydrophobic one was located close to the PP/EVA interface in the EVA phase. For the latter case, no clear interphase of PP/silica/EVA has been observed.[17]

It has been shown[18] that the hydrophobic nanosilica enhances the fibrillation process of LCP in PP/LCP blends. The thickening effect of nanosilica in PP matrix was suggested to be the reason of this observation. Zhang et al.[19] also studied the effect of hydrophobic and hydrophilic nanosilica on PP/LCP blends and reported that only hydrophobic type silica enhances the fibrillation of LCP phase. We investigated the effect of hydrophobic and hydrophilic silica as well as classical compatibilizers on the rheology and morphology of PP/LCP blend in our previous work.[20] Our results showed that SEBS-*g*-MA is more efficient in compatibilizing PP/LCP blend than SEBS, and while hydrophilic silica disperses in both matrix and LCP droplets, the hydrophobic silica concentrates at the interface and PP matrix and enhances the compatibilization of phases. However, it should be noted that the results were limited to only one concentration, 1 wt %, of fumed silica.[20]

In this work, the effects of fumed silica concentration on the rheology and morphology of both PP matrix and PP/LCP blend are studied to provide a deeper insight into compatibilization and/or thickening effect of nanosilica on PP/LCP blend. Studying the rheology of PP/nanosilica system can provide a good basis for understanding the rheology of PP/LCP/nanosilica hybrid blends. It should be noted that we limited our study to blend compositions with dispersed LCP phase in the dilute regime; because such blends have economical application in self-reinforcing composites, and as the volume fraction is below concentrated regime, the hydrodynamic interactions between neighboring LCP droplets can be ignored. The effect of LCP concentration on thermoplastic/LCP blends has been widely investigated in Ref. 9.

In the first part of this work, the aggregation and rheological behavior of hydrophobic and hydrophilic silica filled PP are studied. Then in the second part, the effects of these nanoparticles, as a new potential type of compatibilizers, on the rheology and morphology of PP/LCP blends are studied.

EXPERIMENTAL

Materials

An isotactic PP, Moplen HP500H obtained from Arak petrochemicals, with melt flow rate of 1.8 and a melting point of 165°C, was used as matrix. The dispersed phase was a thermotropic LCP, Vectra A950 (from Hoechst-Celanese, now Ticona) which is a commercial random copolyester of 73% *p*HBA and 27% 4,6-HNA. The as-received pellets had a nominal melting point of 280°C. The nematic–isotropic transition is not known, as it lies above the decomposition temperature.

Fumed nanosilica, Aerosil 200 and Aerosil R816 abbreviated, respectively, as Silica and m-Silica*, were kindly supplied by Degussa GmbH. The hydrophilic nature of the Aerosil 200 powder, which has a specific surface area (BET) of 200 ± 25m^2/g and an average particle size of 12 nm, is due to the presence of silanol groups on its surface. The Aerosil R816 is a hexadecylsilane surface treated hydrophobic nanosilica based on Aerosil 200. The hydrophobic surface treatment changes slightly the specific surface area (BET) to 190 ± 20m^2/g. The nanosilica particles have a spherical surface and are free of pores.

Sample Preparation

Two different series of samples were prepared: (1) PP/Silica and PP/m-Silica nanocomposites and (2) PP/LCP/Silica and PP/LCP/m-Slica hybrid blends. The PP/LCP blend with 85/15 weight fraction was selected to study the effect of nanosilica on its rheology and morphology. Three different weight fraction of silica (1, 2, and 3 wt %) was added during melt blending to this system. If we assume that silica selectively locates in the PP matrix (to be discussed afterward), these compositions correspond to ∼ 1.2, 2.4, and 3.6 weight fractions of silica in PP phase. All samples were prepared by melt blending in a Brabender internal mixer at 290°C and a rotor speed of 60 rpm for approximately 6 min (time to reach a constant torque). To inhibit the thermal degradation during melt blending and rheological measurements, 0.5 wt % Irganox 1076 and Irgafos 168 were added during melt mixing.

Morphological Studies

The transmission electron microscopy (TEM), Philips EM 208 operating at 100 kV was used to study the aggregate size and location of nanosilica in the samples. The samples were prepared using cryomicrotoming (with a diamond knife) at −80°C to prevent any possible morphological changes during cutting.

CamScan model MV2300 scanning electron microscopy (SEM) was used to study the morphology of blend samples. The blend samples were cryofractured in liquid nitrogen and the resulting fractured surfaces were coated with gold before observations by microscope operated at 25.0 kV and under high vacuum.

Rheological Measurements

The rheological measurements were performed with a stress/strain controlled rheometer, Paar Physica model UDS 200,

*The "silica" term is used for both silica types.

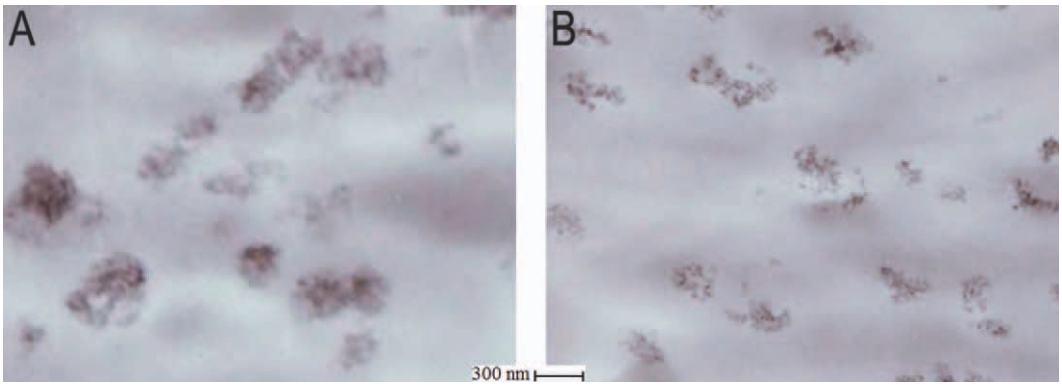

Figure 1. TEM micrograph of (A) PP/hydrophilic silica and (B) PP/hydrophobic silica. [Color figure can be viewed in the online issue, which is available at wileyonlinelibrary.com.]

equipped with parallel plate geometry with 25 mm diameter and 1 mm gap. All the experiments were carried out under a continuous flow of nitrogen gas around the sample pan. The temperature was set at 290°C during experiments in which the LCP is in the nematic state. The frequency sweep tests were performed on samples at strain of 1% which was determined to be in the linear viscoelastic region. Thermal treatment before rheological measurements to achieve a stable nematic state was performed as established by Lin and Winter.[21]

RESULTS AND DISCUSSION

PP Nanocomposites

Typical TEM micrographs of PP filled with hydrophilic and hydrophobic silica are shown in Figure 1. The estimation of aggregate sizes performed for several aggregates in the TEM micrographs of samples shows that the average aggregate sizes in the PP matrix are about 230 nm and 390 nm for hydrophobic and hydrophilic silica filled samples, respectively. The observed higher extent of aggregation for hydrophilic silica is in agreement with the results reported by Aranguren et al.[2] for nanosilica suspensions in polydimethylsiloxane (PDMS).

The effect of nanosilica type and content on the melt linear viscoelastic behavior of the samples is shown in Figure 2. It is seen that the addition of nanosilica even at very low contents increases the viscosity and elasticity of the samples which is a characteristic of nanostructured material. The lowest attainable angular frequency due to thermal stability of samples was about 0.05 rad/s in these measurements. In other words, the high to low frequency sweep experiments were reproducible up to 0.05 rad/s due to thermal degradation of samples.

It can clearly be seen that with increasing silica content of samples, the nonterminal behavior in storage modulus and viscosity upturn at low frequencies become more pronounced. The observed behavior is an indication of three-dimensional physical network formed in these nanocomposite samples. It should be noted that the hydrophilic silica shows higher increase in complex viscosity and storage modulus compared with hydrophobic one which is in agreement with higher extent of aggregation observed in microscopy study.

The results of the melt linear viscoelastic measurements can be used to assess the microstructure of the dispersions. To quantify the percolation threshold, the following percolation model can be used:

$$G' \sim (\varphi - \varphi_{\mathrm{per}})^{v} \tag{1}$$

where v is a power law exponent and φ_{per} is the percolation threshold volume fraction.[2,22] Vermant et al.[23] used a linear–linear plot and approximated the φ_{per} by a linear regression of data points above the percolation. However, using this method yields a lower percolation threshold for hydrophobic silica which does not correlate with rheological trend and morphological observations. Therefore, it seems that fitting the eq. (1) to find the φ_{per} as shown in Figure 3 is more reasonable. The percolation threshold volume fraction was found to be $\sim$ 0.8 and $\sim$ 0.9% for hydrophilic and hydrophobic silica, respectively, which is in agreement with the results reported in the literature for about 1% nanosilica.[24] The slightly lower percolation threshold for hydrophilic silica filled samples is in agreement with its higher extent of aggregation seen in TEM micrographs.

When the particulate networks are above the percolation threshold $\varphi_{\mathrm{per,}}$ the scaling concept of the elastic properties for fractal networks, developed by Shih et al.,[25] can be used to quantitatively analyze the rheological data. Shih et al.[25] considered the structure of a particle network as a collection of fractal aggregates that are elastically linked together. In this case, low frequency solid body response is dominated by the elasticity of the backbones of the aggregates. In this regime, the value of the plateau modulus is predicted to have a power-law dependence on volume fraction:

$$G'_p \sim \varphi^{(3+x)/(3-d_f)} \tag{2}$$

where d_f is the fractal dimension of the aggregate network and x is an exponent that relates the particle volume fraction with aggregate size, that is, x depends on the number of particles per aggregate. According to Potanin,[26] the ratio d_f/x can be considered as an invariant. He proposed $d_f/x = 3/2$ for a three-dimensional network. Although the storage modulus plateau may not

Applied Polymer SCIENCE

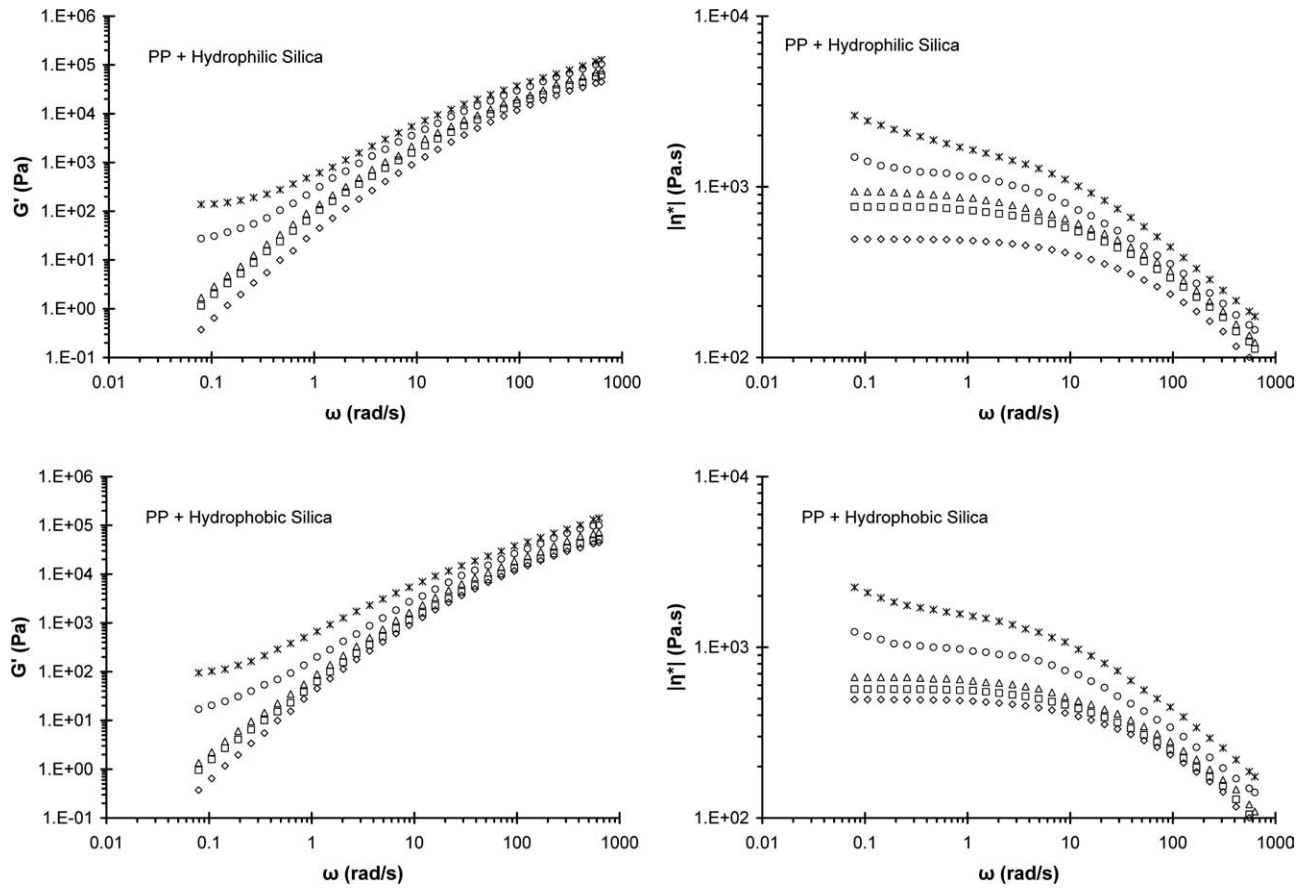

Figure 2. Storage modulus and complex viscosity versus angular frequency of PP nanocomposites with 0 (◇), 1 (□), 1.2 (△), 2.4 (○), and 3.6% (*) silica contents.

always be present in the experimental window, the low frequency storage modulus can be used to study this scaling behavior.[24,27] Figure 4 shows the variations of the low frequency elastic modulus as functions of the solids content. For the hydrophilic silica, power-law exponent was found to be 4.1 which corresponds to fractal dimension $d_f \approx 2$. For the hydrophobic silica, exponent 3.9 is obtained corresponding to $d_f \approx 1.9$. The lower value of fractal index for the m-Silica containing samples can be explained by a structure which is less dense than that of the Silica ones. The obtained fractal dimensions correspond to chemically limited aggregation interaction type and are in agreement with the results of Khan et al.[3] and Yziquel et al.[4]

The lower percolation threshold and hence higher aggregation tendency of hydrophilic silica may be explained by its lower affinity with PP and hydrogen bonding tendency between particles in comparison to hydrophobic silica. However, considering fundamental theories concerned with particle interactions in

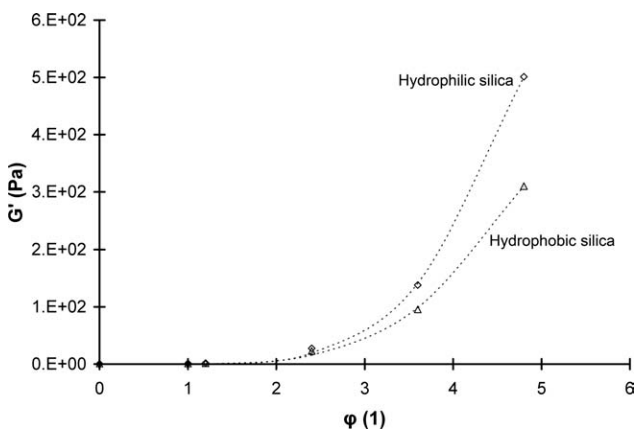

Figure 3. The fitting of eq. (1) for nanosilica filled samples.

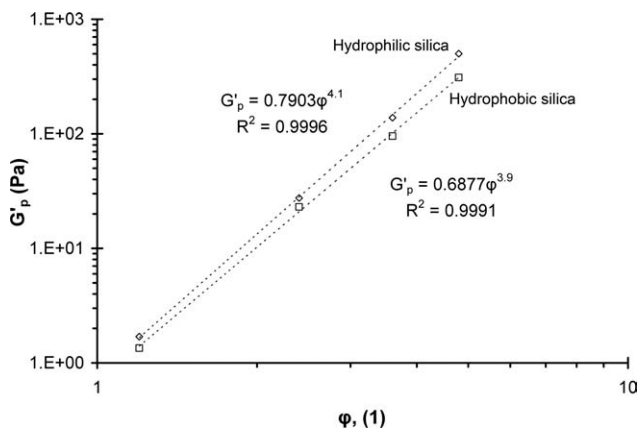

Figure 4. The fitting the power-law model on the storage modulus versus volume fraction dependency.

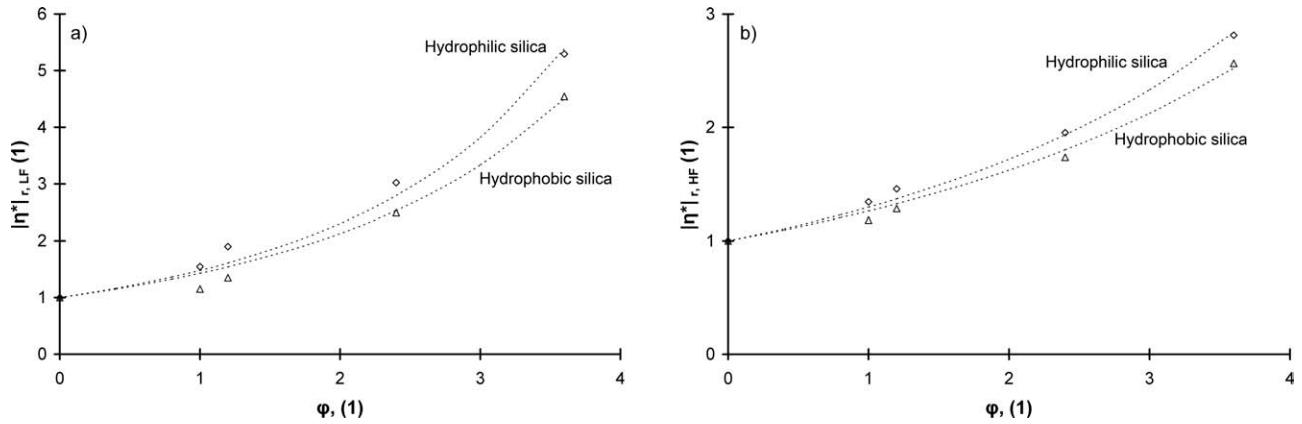

Figure 5. The fitting of Krieger-Dougherty equation at (a) low frequency and (b) high frequency

terms of electrostatic, Van der Waals, and steric forces[28] can be more helpful. The electrostatic repulsion results from the overlapping of the electric double layer that develops at charged interfaces. In the simplest case, a repulsive force develops between the interfaces due to the entropic confinement of the counter-ions which neutralize a charged interface.[28] The neutral nature of polymeric media (the absence of ions) and uncharged interface of nanosilica implies insignificant electrostatic interaction. According to the microscopic theory by Hamaker, the Van der Waals interaction between two macroscopic bodies can be found by the integration of Van der Waals interaction between molecules over all couples of molecules.[28] The presence of silanol groups at the surface of hydrophilic silica compared to the hexadecyl chain at the surface of m-Silica results in stronger dipoles and hence stronger Van der Waals attraction between particles.[28] On the other hand, hexadecyl chains attached to the surface of hydrophobic silica cause higher degree of steric repulsion between particles of hydrophobic silica. Therefore, the higher degree of aggregation and denser aggregates of hydrophilic silica compared with hydrophobic one are expected.

For concentrated hard sphere suspensions, the Krieger and Dougherty equation[29] is suitable to describe the relationship between the relative viscosity and the volume fraction of solid particles:

$$\eta_r = \frac{\eta}{\eta_m} = \left(1 - \frac{\varphi}{\varphi_m}\right)^{-[\eta]\varphi_m} \quad (3)$$

where η_r is the relative viscosity of filled polymer with respect to the matrix, φ_m is the maximum packing fraction, and $[\eta]$ is the intrinsic viscosity of suspensions. This equation has been used at both low and high shear rates of viscosity obtained from flow curve measurement,[30] and for storage and loss moduli at low or high frequencies as suggested by Vermant et al.[23] Although the low frequency viscoelasticity mainly gives information about the aggregates and eventually the percolating structure formed by the aggregates, the high frequency viscoelasticity is dominated by the polymeric matrix contributions due to an increase of hydrodynamic contribution of matrix. In the present work, both low and high frequency complex viscosities of samples were fitted to the Krieger and Dougherty equation, as shown in Figure 5. It is seen that the model fits quite well, and consequently it can predict the relative viscosity at various volume fractions.

The results (summarized in Table I) show that φ_m of hydrophilic silica is lower than that of hydrophobic one indicating that the former reaches the closest packing at lower volume fractions. Higher value of $[\eta]$ for hydrophilic silica filled samples is expected due to its higher thickening effect observed in Figure 2. Similar results are presented by Chen et al.[30] for suspension of silica particles in mineral oil. Although the maximum packing fraction (φ_m) was found to be close to the theoretical value (0.74) for the microparticles, for the nanosilica filled samples the values were in the range of 0.07–0.22 that is comparable to our results.[30] The lower φ_m of nanoparticles was attributed to the formation of branched aggregates by Chen et al.[30] Higher value of $[\eta]$ for hydrophilic silica corresponds to the higher aspect ratio of aggregates[31] which could be the reason of lower φ_m value of this silica type.

Higher φ_m and lower $[\eta]$ values at high frequencies compared with low frequency results are observed (Table I). Similar results were obtained by Chen et al.[30] in two different shear rates which were attributed to the breakage of the branched, agglomerated structure into smaller structures under high shear forces and thus relatively tighter packing structures. Although there is hardly breakage of aggregates in the small amplitude oscillatory shear flow compared to the shear forces in rotational flow, the higher φ_m and lower $[\eta]$ values at high frequencies can be attributed to the dominated hydrodynamic contributions of

Table I. The $[\eta]$ and φ_m Obtained from Krieger-Dougherty Equation

	$[\eta]_{LF}$[a]	$\varphi_{m,\ LF}$	$[\eta]_{HF}$[b]	$\varphi_{m,\ HF}$
Hydrophilic silica	37.1	0.094	25.1	0.140
Hydrophobic silica	34.0	0.103	22.6	0.155

[a]LF index is corresponding to low frequency data, [b]HF index is corresponding to data taken at high frequencies.

polymeric matrix and less contribution of three-dimensional network between aggregates.

Blend nanocomposites

The thermodynamic preference of filler to distribute selectively can be predicted by introducing a wetting coefficient, W_a[32]:

$$W_a = \frac{\gamma_{\text{filler-B}} - \gamma_{\text{filler-A}}}{\gamma_{\text{A-B}}} \quad (4)$$

where $\gamma_{\text{filler-A}}$and $\gamma_{\text{filler-B}}$are the interfacial tensions between the filler and polymer A or B, respectively, and $\gamma_{\text{A-B}}$ is the interfacial tension between polymer A and B. If $W_a > 1$, the filler is located within A-phase, if $-1 < W_a < 1$, the filler concentrates at the interface, and if $W_a < -1$, the filler is selectively distributed in the B-phase. In our previous work,[20] we found that at thermodynamic equilibrium, the hydrophilic silica particles should be preferentially located in the LCP phase, whereas the hydrophobic silica should be concentrated at the interface in this hybrid system.

By using TEM analysis, we showed that while hydrophobic silica is located at the interface and in the PP matrix, hydrophilic silica is distributed in both phases.[20] These results were in agreement with the experimental results reported by Zhang et al.[19] By considering this result and those predicted by thermodynamic approach, one may notice that there is some inconsistency between the experimental and theoretical results. This discrepancy can be explained in terms of the concentration effect, significance of diffusion by Brownian motion or convective forces, and/or temperature effects on interfacial properties. By estimating the required amount of nanoparticle to cover dispersed droplets, we found that 0.1% of hydrophobic silica is enough to saturate whole PP/LCP interface if it works as a compatibilizer.[20] This is evidenced by TEM micrograph which shows a fraction of hydrophobic silica particles tends to locate in the PP phase after saturation of interface.[20]

The time required for a particle with radius r (in this case an aggregate) to diffuse a distance of its radius can be expressed as in Ref. 33:

$$t_D = \frac{r^2}{D_s} \quad (5)$$

where $D_s(\varphi)$ is the short time self-diffusion coefficient which reduces to the following equation for a dilute suspension of spherical droplets:

$$D_0 = \frac{k_B T}{6\pi\eta r} \quad (6)$$

In this equation, k_B is the Boltzmann constant, and η is the viscosity of media at temperature T and shear rate imposed on the sample. The viscosity of the melt blend was calculated at operational conditions of internal mixer (in which the shear rate was found to be about 52 s^{-1} [Ref. 34]). It is estimated that aggregates need 17–145 min to diffuse a distance equal to their size. Therefore, it is evident that Brownian motion is too slow to affect the positioning of aggregates in PP/LCP blend during melt mixing.

The frequency of collision between particles per unit volume and unit time in simple shear flow with shear rate $\dot{\gamma}$ can be described as follows in Ref. 35:

$$C = \frac{2}{3}\dot{\gamma}\, d^3 n^2 \quad (7)$$

where n is the number of particles with size d per unit volume. As the volume fraction of particles is $\varphi = n\frac{\pi}{6}d^3$, this equation can be rewritten as follows:

$$C = \frac{24\dot{\gamma}\varphi^2}{\pi^2 d^3} \quad (8)$$

It should be noted that this equation was not developed for hybrid systems; however, it can provide an estimation of convective diffusion during the melt mixing process. Therefore, it can be estimated that 4.6×10^{13} collisions take place between dispersed phase particles during the mixing in the internal mixer. This estimation shows that while the Brownian motion has negligible effect on the diffusion of particles to the interface of LCP droplets, very high rate of convective migration compensates this slow thermodynamic diffusion. The significance of convective diffusion compared to Brownian motion can be verified by Peclet number as well. The Peclet number is defined as the ratio of the time required for a droplet to diffuse a distance of its radius, t_D, divided by the time required for it to convect the same distance, $1/\dot{\gamma}$:

$$\text{Pe} = \frac{\dot{\gamma} r^2}{D_s(\varphi)} \approx \frac{6\pi\eta\dot{\gamma} r^3}{k_B T} \quad (9)$$

The calculations show that Peclet number is much higher than 1, which means that the convective mechanism is dominant during the melt mixing process. According to the above discussion, the discrepancy between wetting parameter prediction and morphological observation in Ref. 20 can be explained as follows:

- For hydrophobic silica which prefers to concentrate at the interface, the used concentrations of fumed silica are much higher than interface saturation. Hence, the excess particles will stay in the more hydrophobic PP phase after saturation of interface.
- Although hydrophilic silica should be preferentially located in the LCP phase, it can be found in both phases. This could be due to the low saturation concentration of silica in the dispersed phase with liquid crystalline structure. In other words, if the LCP droplet collide with silica aggregates, it will be wetted by LCP phase (see TEM micrographs in Ref. 20), but further diffusion inside the LCP droplet may not be preferable due to the crystalline structure.

The comparison of aggregate sizes between the PP/LCP blends and PP nanocomposites does not show a considerable difference which may be due to the insignificant effect of LCP dispersed

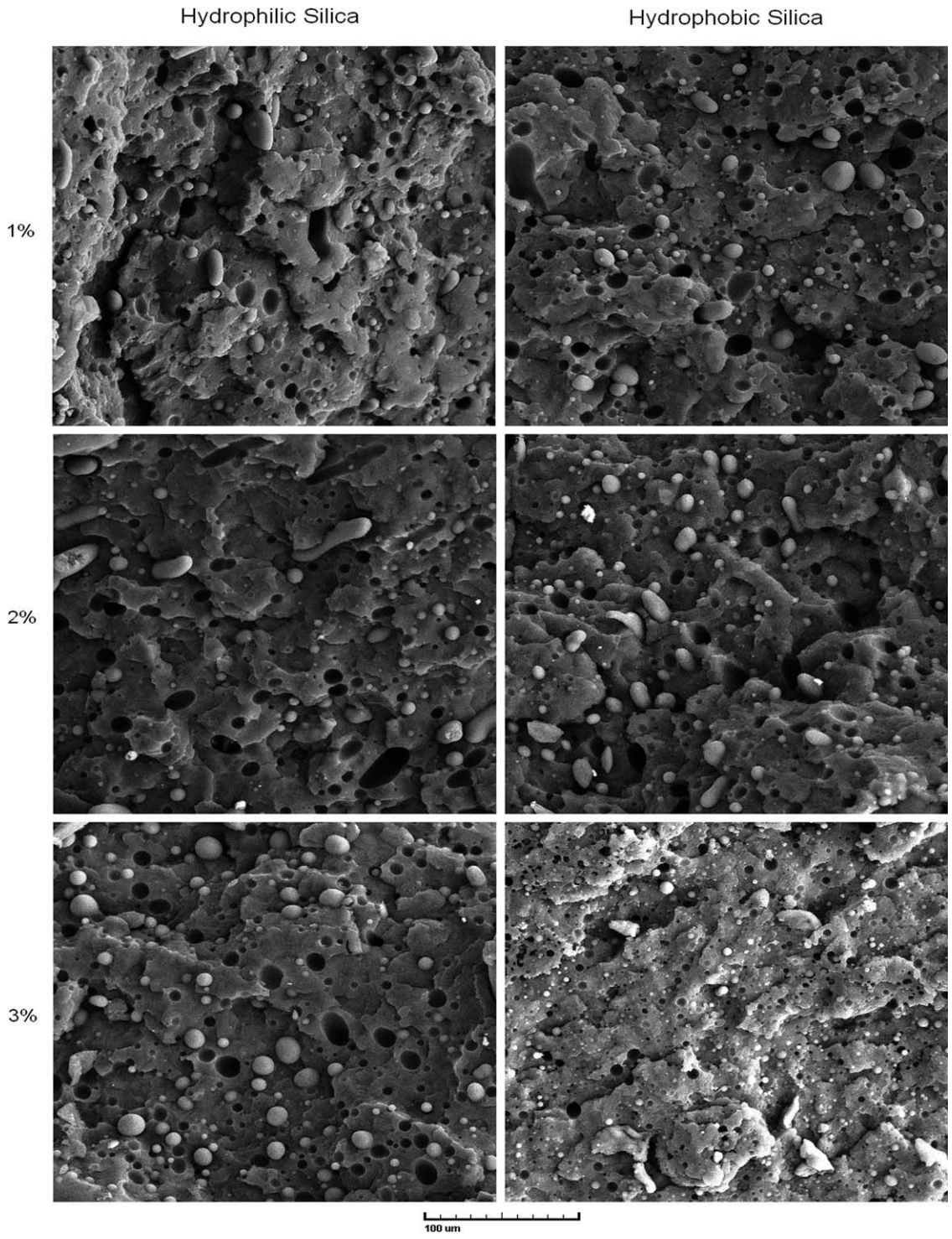

Figure 6. The SEM micrographs of PP/LCP/silica hybrid samples.

phase on aggregate size, calculation errors, and/or the local characteristic of TEM images.

SEM micrographs of PP/LCP hybrid blends are shown in Figure 6. As it is clearly seen, the LCP minor phase in the form of nearly spherical droplets is distributed in PP matrix. However, for samples containing 1 and 2% nanosilica, more nonspherical droplets are seen compared to 3% silica containing PP/LCP blends. This can be explained by local barrier effect of nanosilica aggregates at lower concentration that will be compensated by more uniform local distribution of aggregates at higher concentrations. For a quantitative analysis, the droplet size was determined by using image analysis. Typically, 300 particles were analyzed per sample and the number average radius $\bar{R}_N$ and volume average radius $\bar{R}_V$ of dispersed phase were

Applied Polymer SCIENCE

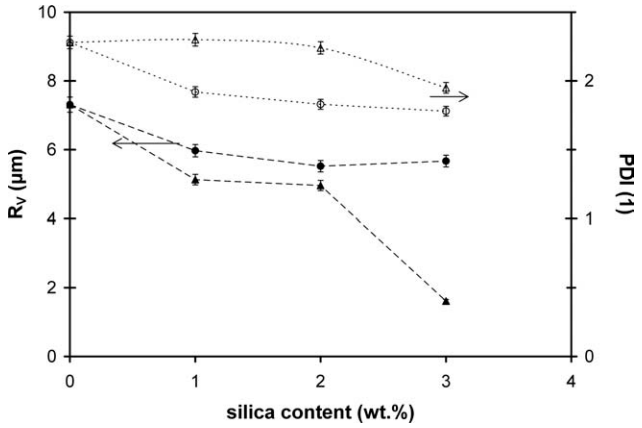

Figure 7. Droplet size and its distribution for PP/LCP blends with different: (▲, △) hydrophobic, and (●, ○) hydrophilic silica contents.

calculated by assuming the dispersed phase as spherical particles by following equations:

$$\bar{R}_N = \frac{\sum n_i R_i}{\sum n_i} \tag{10}$$

$$\bar{R}_V = \frac{\sum n_i R_i^4}{\sum n_i R_i^3} \tag{11}$$

It should be noted that in the emulsion theories, the domain size is usually expressed as volume average radius. The polydispersity index (PDI), of droplet size distribution can be estimated in terms of $\bar{R}_V/\bar{R}_N$ ratio. For a monodisperse system, this ratio tends to unity and the values greater than one show the broader droplet size distributions.

The values of droplet size and polydispersity of LCP dispersed phase in hybrid samples are shown in Figure 7. These results show that the addition of nanosilica results in reduction of the droplet size during melt blending, although their effect on the polydispersity is rather complicated to draw a clear conclusion.

Incorporation of nanofiller in a polymer blend sample can reduce the droplet size by three different mechanisms:

(a) reducing the viscosity ratio by thickening the matrix[19,36]
(b) suppressing the coalescence during mixing[27,37]
(c) compatibilization by concentrating at the interface[16,37–39]

Note that the mechanisms (b) and (c) are not completely independent, because besides the hindrance of coalescence by solid aggregates, the presence of compatibilizer at the interface also results in suppression of coalescence.[12] Nanosilica is especially known as a thickening agent in the emulsion and suspension systems. Zhang et al.[19] attributed the smaller droplet size of PP/LCP blend in the presence of nanosilica to the thickening effect, although they did not systematically differentiate the hydrophobic and hydrophilic ones. However, we showed that while the hydrophilic silica has higher thickening capability according to the results obtained in PP nanocomposites section, higher degree of droplet size reduction is observed for hydrophobic silica filled blend samples. This suggests that other phenomena control the final droplet size of blend samples. In other words, the existence of m-Silica at the interface of prepared PP/LCP blend, its weaker thickening effect and smaller resultant droplet size of m-Silica filled blend samples compared to hydrophilic silica filled ones confirm a compatibilization effect of m-Silica for this system in accordance to our previous work.[20]

From the three mechanisms mentioned above, both hydrophilic and hydrophobic silica can induce coalescence hindrance and thickening effect. The coalescence can be hindered by the presence of aggregates in the matrix or particles at the interface. The bigger aggregates of hydrophilic silica imply higher extent of coalescence hindrance in comparison to hydrophobic one. The results discussed earlier showed that hydrophilic silica has higher extent of thickening effect on the viscosity of PP nanocomposites. It should be noted that small amount of hydrophilic silica in LCP droplets was also observed which can affect the viscosity ratio. However, it can be suggested that the viscosity ratio has insignificant effect on the final droplet size, as the presence of extensional flow field in the internal mixer[40] can control the droplet break-up process. Therefore, considering only coalescence hindrance and thickening mechanisms suggest smaller droplet size for hydrophilic silica containing blend samples. However, the morphological studies showed the opposite trend. Thus, the compatibilizing effect of hydrophobic silica can be the mechanism which controls the final morphology of PP/LCP/m-Silica hybrid samples.

If an additive acts as a thickening agent, it is expected to enhance the shear stress transfer particularly in low shear rate region—where the greater droplet size exists—and therefore it will lead to a narrower droplet size distribution. This reveals that the hydrophobic silica has not appreciable thickening effect on PP/LCP blend (at least in 0–2 wt % silica content range), because it does not affect the PDI in this range. This result supports the compatibilization effect of hydrophobic nanosilica which decreases the mean droplet size more than hydrophilic one. The reduced LCP droplet size and polydispersity for hydrophilic silica containing blend samples can be attributed to the thickening effect of this silica and hindrance effect of aggregates on coalescence process.

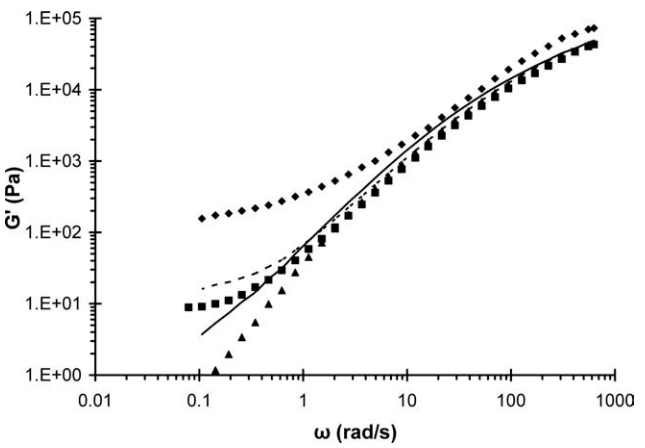

Figure 8. The storage modulus of PP (▲), LCP (◆), PP/LCP blend (■), and the prediction of mixing rule (---) and Palierne's model (—).

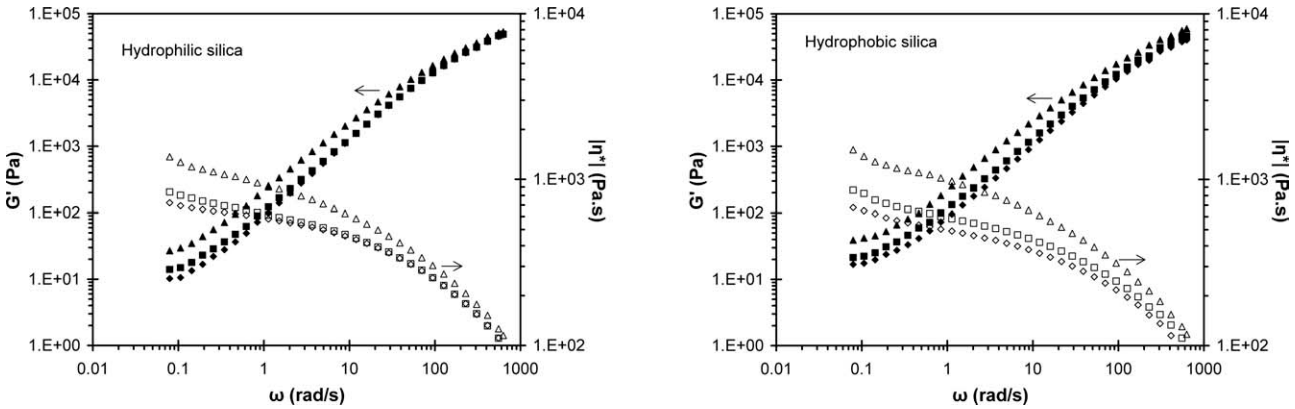

Figure 9. The rheological behavior of (◊) 1, (□) 2, and (△) 3wt.% silica filled PP/LCP blend.

The abrupt reduction in LCP droplet size after 2 wt % for hydrophobic silica filled blend is matching the range of percolation volume fraction in the PP matrix. Although the concentration of hydrophilic silica in 3 wt % containing PP/LCP is also above the percolation threshold, we do not see any further refinement in this blend sample. This suggests that the concentration of a particulate compatibilizer should be higher than percolation threshold to achieve high efficiency in droplet refinement.

Figure 8 shows the storage modulus, G′, as a function of angular frequency for PP, LCP, and PP/LCP blend samples. It is seen that LCP exhibits greater melt elasticity compared with PP matrix at whole frequency range. The storage modulus plateau of LCP at low frequencies is attributed to the solid body behavior resulted from the highly ordered nematic state close to the melting point. The G' of PP/LCP blend sample is compared with simple mixing rule and Palierne's model in Figure 8. The results show a negative deviation from simple mixing rule due to weak interfacial adhesion between PP and LCP phases. The Palierne's advanced model[41] was found to be unable to predict the rheological behavior of LCP containing blend, in accordance to the literature.[8] The pronounced nonterminal behavior of PP/LCP blend sample, indicating longer relaxation time of dispersed droplets compared to Palierne's model[41] prediction, could originate from internal structure of LCP droplets.

The linear viscoelastic properties of silica containing PP/LCP blend samples are shown in Figure 9. As seen, the extent of increase in G′ and $|\eta^*|$ with increasing silica content is higher for hydrophobic silica compared with hydrophilic one. This supports the compatibilization of hydrophobic silica which has lower thickening ability and smaller aggregates to hinder the coalescence process. As it was shown in Figure 8, the Palierne's model could not be used to predict the rheological behavior of simple PP/LCP blend sample when the interfacial tension is known and *vice versa*. Similar behavior was found for silica containing blend samples. Vermant et al.[27] suggested that for estimating the ratio of droplet size to interfacial tension for nanosilica containing blend, the interface contribution can be obtained by subtracting the matrix and dispersed phase contribution; and then the crossover frequency between G'_{INT} and G''_{INT} can be used to estimate this ratio. However, in the present work, the observed negative deviation from mixing rule

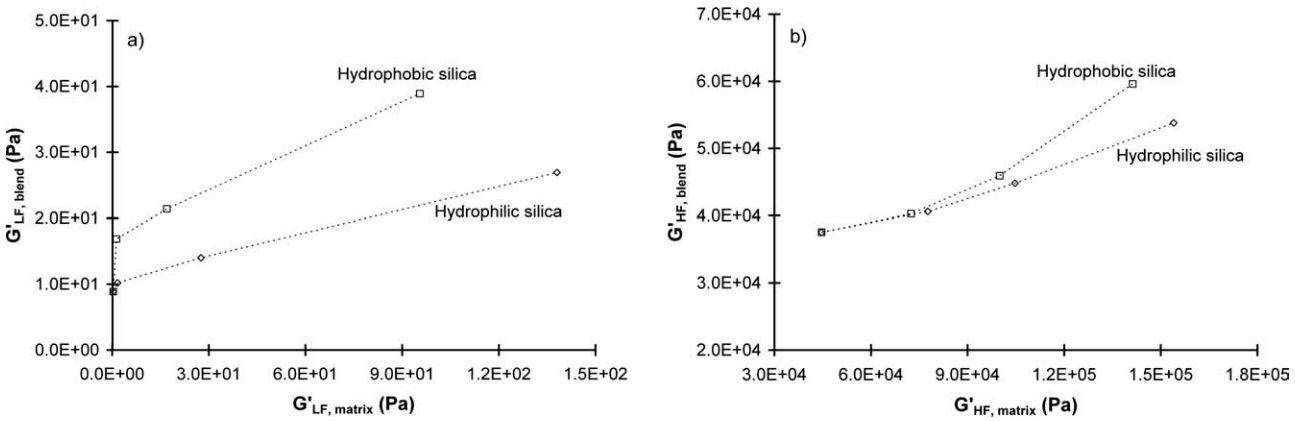

Figure 10. Variation of storage modulus of PP/LCP/silica samples versus storage modulus of PP/silica nanocomposites at (a) low frequency and (b) high frequency.

shows that both G'_{INT} and G''_{INT} are negative in the whole frequency range for all blend samples. Therefore, neither the Palierne's model is able to predict the rheological behavior of hybrid samples, nor the Vermant et al.'s method can be applied for estimation of interfacial tension between PP and LCP in the presence of nanoparticles. It means that an advanced model or new experimental methods should be developed to describe this behavior.

Results in Figure 9 can be presented in terms of storage modulus variation of PP/LCP/silica samples versus corresponding G′ values of PP/silica nanocomposites at low and high frequencies (Figure 10). It is seen that the presence of LCP phase in hydrophobic silica containing blend samples results in higher extent of elasticity at both low and high frequencies. The higher order of elasticity at high frequency for hydrophobic silica, where the molecular scale contributions are significant, shows the enhanced stress transfer from matrix to dispersed phase at molecular scale. At low frequency, the contributions of interfacial energy of dispersed droplets (microscale contributions) are significant and thus the higher order of elasticity for hydrophobic silica containing blend samples suggests higher order of droplet deformation due to enhanced interfacial adhesion. Therefore, higher degree of compatibility between PP and LCP is achieved in the presence of hydrophobic silica compared with hydrophilic one.

CONCLUSION

The rheology and morphology of nanosilica containing PP and PP/LCP blend were studied. The rheological results were used to calculate the percolation threshold, fractal index, and the intrinsic viscosity of PP/silica nanocomposites. It was found that hydrophobic silica has higher tendency for aggregation and forms bigger and denser aggregates. The lower percolation threshold and the higher fractal dimension for hydrophilic silica are due to its stronger particle–particle interaction rather than polymer–particle interaction compared with hydrophobic one. Although the hydrophobic silica has lower thickening capability and lower coalescence hindrance caused by aggregates, it locates at the interface of PP/LCP blend and results in smaller droplet size and higher elasticity in comparison to hydrophilic silica. It was found that the concentration of a particulate compatibilizer should be higher than percolation threshold to achieve high efficiency in droplet refinement. The results suggest that the hydrophobic silica has a compatibilization capability for PP/LCP blend, whereas the hydrophilic silica mostly works as a thickening agent and suppresses the coalescence. We found that the stress transfer at molecular scale and droplet deformation due to enhanced interfacial adhesion is enhanced by hydrophobic silica more than hydrophilic one.

REFERENCES

1. Cassagnau, P. *Polymer* **2008,** *49*, 2183.
2. Aranguren, M. I.; Mora, E.; DeGroot, J. V.; Macosko, C. W. *J. Rheol.* **1992,** *36*, 1165.
3. Khan, S. A.; Zoeller, N. J.; *J. Rheol.* **1993,** *37*, 1225.
4. Yziquel, F.; Carreau, P. J.; Tanguy, P. A. *Rheol. Acta* **1999,** *38*, 14.
5. Sternstein, S. S.; Zhu, A.-J. *Macromolecules* **2002,** *35*, 7262.
6. Aranguren, M. I.; Mora, E.; Macosko, C. W. *J. Colloid Interface Sci.* **1997,** *195*, 329.
7. Kim, W. N.; Denn, M. M. *J. Rheol.* **1992,** *36*, 1477.
8. Riise, B. L.; Mikler, N.; Denn, M. M. *J. Non-Newtonian Fluid Mech.* **1999,** *86*, 3.
9. Hashmi, S. A. R.; Kitano T. *Appl. Rheol.* **2007,** *17*, 64510.
10. Datta, D.; Baird, D. G. *Polymer* **1995,** *36*, 505.
11. O'Donnell, H. J.; Baird, D. G. *Polymer* **1995,** *36*, 3113.
12. Harrats, C.; Thomas, S.; Groeninckx, G., Eds. Micro- and Nanostructured Multiphase Polymer Blend Systems: Phase Morphology and Interfaces; CRC Press, Taylor & Francis Group: Boca Raton, **2006.**
13. Lipatov, Y. S. Polymer Reinforcement; ChemTec Publishing: Toronto, Canada, **1995.**
14. Zhang, Q.; Yang, H.; Fu, Q. *Polymer* **2004,** *45*, 1913.
15. Ray, S. S.; Pouliot, S.; Bousmina, M.; Utracki, L. A. *Polymer* **2004,** *45*, 8403.
16. Elias, L.; Fenouillot, F.; Majeste, J. C.; Cassagnau, P. *Polymer* **2007,** *48*, 6029.
17. Elias, L.; Fenouillot, F.; Majesté, J. C.; Alcouffe, P.; Cassagnau, P. *Polymer* **2008,** *49*, 4378.
18. Lee, M. W.; Hu, X.; Yue, C. Y.; Li, L.; Tam, K. C.; Nakayama, K. *J. Appl. Polym. Sci.* **2002,** *86*, 2070.
19. Zhang, L.; Tam, K. C.; Gan, L. H.; Yue, C. Y.; Lam, Y. C.; Hu, X. *J. Appl. Polym. Sci.* **2003,** *87*, 1484.
20. Foudazi, R.; Nazockdast, H. *Appl. Rheol.* **2010,** *20*, 12218.
21. Lin, Y. G.; Winter, H. H. *Macromolecules* **1988,** *21*, 2439.
22. Rueb, C. J.; Zukoski, C. F. *J. Rheol.* **1997,** *41*, 197.
23. Vermant, J.; Ceccia, S.; Dolgovskij, M. K.; Maffettone, P. L.; Macosko, C. W. *J. Rheol.* **2007,** *51*, 429.
24. Paquien, J.-N.; Galy, J.; Gérard, J.-F.; Pouchelon, A. *Colloids Surf. A* **2005,** *260*, 165.
25. Shih, W. H.; Shih, W. Y.; Kim, S. I.; Aksay, A. I. *Phys. Rev. A* **1990,** *42*, 4772.
26. Potanin, A. A. *J. Colloid Interface Sci.* **1991,** *145*,140.
27. Vermant, J.; Cioccolo, G.; Golapan Nair, K.; Moldenaers, P. *Rheol. Acta* **2004,** *43*, 529.
28. Israelachvili, J. N. Intermolecular and Surface Forces; Academic Press, London, **1992.**
29. Krieger, I. M.; Dougherty, T. J. *Trans. Soc. Rheol.* **1959,** *3*, 137.
30. Chen, S.; Øye, G.; Sjoblom, J. *J. Dispersion Sci. Technol.* **2005,** *26*, 791.
31. Brenner, H. *Int. J. Multiphase Flow* **1974,** *1*, 195.

32. Sumita, M.; Sakata, K.; Asai, S.; Miyasaka, K.; Nakagawa, H. *Polym. Bull.* **1991,** *25*, 265.
33. Elias, L.; Fenouillot, F.; Majeste, J. C.; Martin, G.; Cassagnau, P. *J. Polym. Sci. Part B: Polym. Phys.* **2008,** *46*, 1976.
34. Bousmina, M.; Ait-Kadi, A.; Faisant, J. B. *J. Rheol.* **1999,** *43*, 415.
35. Chesters, A. K. *Chem. Eng. Res. Des.,* **1991,** *69*, 259.
36. Chen, J.; Chen, P.; Wu, L.; Zhang, J.; He, J. *Polymer* **2007,** *48*, 4242.
37. Zhanga, B.; Dinga, Y.; Chena, P.; Liua, C.; Zhanga, J.; Hea, J.; Hu, G.-H. *Polymer* **2005,** *46*, 5385.
38. Pisharath, S.; Hu, X.; Wong, S. C.; *Compos. Sci. Technol.* **2006,** *66*, 2971.
39. Fenouillot, F.; Cassagnau, P.; Majeste, J.-C. *Polymer* **2009,** *50*, 1333.
40. Manas-Zloczower, I.; Tadmor, Z., Eds., Mixing and Compounding of Polymers—Theory and Practice; Hanser: New York, **1994.**
41. Palierne, J. F. *Rheol. Acta* **1991,** *29*, 204.